Multiple Curvatures in a Tendon-Driven Continuum Robot Using a Novel Magnetic Locking Mechanism

Chloe Pogue, Priyanka Rao, Quentin Peyron, Jongwoo Kim, Jessica Burgner-Kahrs, Eric Diller

Multiple Curvatures in a Tendon-Driven Continuum Robot Using a Novel Magnetic Locking Mechanism

Chloe Pogue[1,2,5], *Student Member, IEEE*, Priyanka Rao[2,5], *Student Member, IEEE,*
Quentin Peyron[2,3], Jongwoo Kim[2,4], *Member, IEEE*,
Jessica Burgner-Kahrs[2,5], *Senior Member, IEEE*, and Eric Diller[1,5], *Senior Member, IEEE*

***Abstract*— Tendon-driven continuum robots show promise for use in surgical applications as they can assume complex configurations to navigate along tortuous paths. However, to achieve these complex robot shapes, multiple segments are required as each robot segment can bend only with a single constant curvature. To actuate these additional robot segments, multiple tendons must typically be added on-board the robot, complicating their integration, robot control, and actuation. This work presents a method of achieving two curvatures in a single tendon-driven continuum robot segment through use of a novel magnetic locking mechanism. Thus, the need for additional robot segments and actuating tendons is eliminated. The resulting two curvatures in a single segment are demonstrated in two and three dimensions. Furthermore, the maximum magnetic field required to actuate the locking mechanism for different robot bending angles is experimentally measured to be $6.1\,\mathrm{mT}$. Additionally, the locking mechanism resists unintentional unlocking unless the robot assumes a 0° bending angle and a magnetic field of $18.1\,\mathrm{mT}$ is applied, conditions which are not typically reached during routine use of the system. Finally, addressable actuation of two locking mechanisms is achieved, demonstrating the capability of producing multiple curvatures in a single robot segment.**

I. Introduction

Continuum robots have been widely used for minimally invasive surgeries due to their dexterity and small dimensions [1]. They can bend in curvilinear shapes, allowing them to access constricted spaces and to perform surgical tasks. Tendon actuation is one of the common modes of actuation for these robots, with tendons routed alongside an axially stiff backbone. Tendon driven continuum robots (TDCRs) have tendons terminating at the end of a segment and are actuated by motors placed at the base, actuating each segment by pulling or releasing these tendons [2]. Actuating them extrinsically, with motors placed outside the deformable robot shape, allows for smaller diameter robots. The tendons are commonly routed parallel to the incompressible backbone, following a straight line. On actuation, each segment generally bends following an approximate constant curvature arc in 3D, and bending is typically accomplished using three or more tendons. Achieving variation in curvature along the robot in free space requires more than a single segment. Each segment requires a minimum of two motors with a pair of antagonistic tendons to actuate it in 3D space. Stacking multiple segments complicates the actuation unit due to complex routing that requires higher integration efforts, as well as the required control algorithms for synchronization and trajectory generation. It also results in a bulky actuation system and increased frictional forces.

Achieving multiple curvatures has been implemented through various design modifications other than using multiple segments. For example, non-straight tendon routing [3]–[5] allows a single segment to bend with varying curvature. While these prior works consider tendons routed at a constant distance from the backbone, varying this distance has also been studied to obtain variable curvatures [6], [7]. Liu et al. [8] use multiple nitinol slices assembled under a steel shell to achieve an S-shaped curve.

Another possible method of achieving multiple curvatures is to use locking/latching mechanisms. They can be used to grip moving parts in the robot and prevent their relative motion in certain portions, resulting in restricted deformations. Hence, they can be used to control the curvature at multiple points. A definition of locking mechanisms in robotics is provided by Plooij et al. [9] as devices that allow and prevent motion between parts. The designs proposed for use in continuum robots can be classified into two major categories [9], based on their friction-based or mechanical locking principle. The use of locking mechanisms to achieve multi-curvature capability offers the advantage of being modular and have smaller sizes compared to the robot. They can be used as actively actuated components to change the robot shape, as opposed to passive design modifications to the backbone or tendon routing.

Friction-based mechanisms use high friction to lock the system. SMA springs are used [10] to vary the internal friction between the backbones and disks. A friction material is used to coat the moving parts [11] to arrest sliding between two flexible concentric backbones. Bishop et al. [12] also proposed a friction-based mechanism which uses SMA wires to increase the friction between clutches and beaded tendons,

This work was supported by the XSeed funding program of the Faculty of Applied Science & Engineering at the University of Toronto and the University of Toronto Mississauga. (*Corresponding author: Chloe Pogue. Email:* chloe.pogue@mail.utoronto.ca)

[1]Microrobotics Lab, Department of Mechanical and Industrial Engineering, University of Toronto, 5 King's College Rd, Toronto, ON M5S 3G8.

[2]Continuum Robotics Laboratory, Department of Mathematical & Computational Sciences, University of Toronto, Mississauga, ON, Canada.

[3]DEFROST team, Inria Lille-Nord Europe and CRIStAL UMR CNRS 9189, University of Lille, Villeneuve d'Ascq, France.

[4]Biomedical & Intelligent Robotics Laboratory, Department of Mechanical Engineering, Kyung Hee University, Republic of Korea.

[5]Robotics Institute, University of Toronto, Myhal Centre for Engineering Innovation & Entrepreneurship, Toronto, ON, Canada.

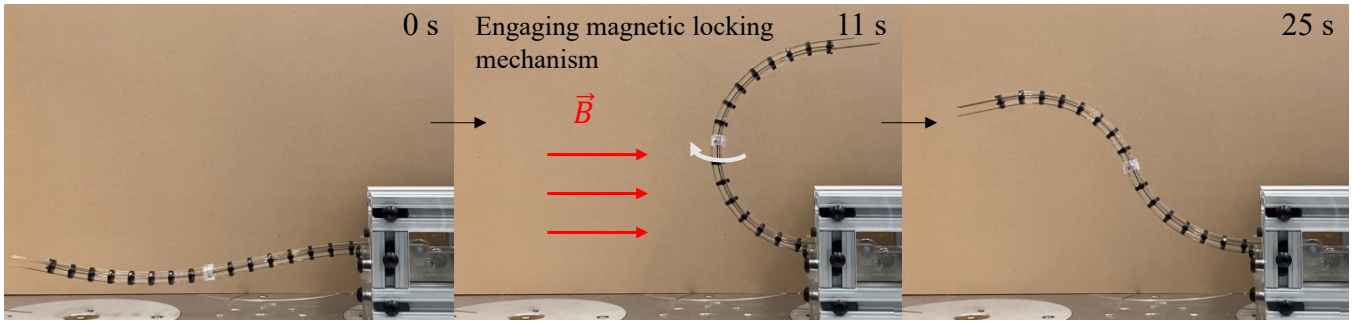

Fig. 1: Locking process: The robot is unlocked in its starting configuration (0s). The robot is bent and a magnetic field is applied to engage the magnetic locking mechanism. The white arrow indicates the rotation direction of the locking mechanism (11s). The magnetic locking mechanism is locked enabling two curvatures in the robot (25s).

locking the shape of a portion of the robot. Piezoelectric actuators are used [13] to clamp on to backbones. These actuators are used for shape-locking to achieve follow-the-leader deployment. Mechanical mechanisms use a mechanical structure to obstruct motion. For example, Sun et al. [14] used a locking mechanism consisting of a rotating cam which pushes against an elastic rod to switch between pneumatic and elastic rod actuation. A clutch and a parallel mechanism are used [15] to create a locking mechanism for follow-the-leader deployment. Vacuum pressure is used to lock the backbone [16] by engaging flexible toothed links that prevent the backbone from bending.

To achieve multiple curvatures, a wireless locking mechanism which allows tools to be routed through the TDCR is essential for surgical applications. The existing locking mechanisms often require a constant power source for actuation which can cause the robot to reach elevated temperatures and be harmful to the patient. Furthermore, the proposed locking mechanisms are usually tethered as electrical wires or pneumatic conduits must be fed through the robot's body to provide energy to the mechanism. In addition, friction-based locking mechanisms have higher energy consumption.

A locking mechanism based on magnetic actuation provides a possible alternative to the above. Magnetic actuation has already been well researched in the robotics community for surgical interventions (e.g. [17]). Magnetic fields can safely penetrate human tissues and can be used for wireless actuation. To the best of our knowledge, achieving multiple curvatures in a single TDCR segment has yet to be achieved through magnetic actuation. In this work, we propose a novel magnetically-actuated locking mechanism (MLM) on board a TDCR to enable multiple curvatures in a single robot segment, thus eliminating the need for additional robot segments and supplementary actuating tendons (Fig. 1). Due to the magnetic actuation, the proposed locking mechanism is untethered, allowing for backbone and actuation unit miniaturization, can be rapidly actuated, and the actuating magnetic fields are safe for use in surgical tasks. A modified version of the torsional spring presented in [18] is embedded into the MLM allowing it to switch between stable locked and unlocked states wirelessly, eliminating the need for a constant power supply. It is a mechanical locking mechanism, and thus uses less energy than friction based designs.

The contributions of this paper are as follows. First, we propose a novel design for a MLM and TDCR. Second, we demonstrate the locking mechanism's ability to achieve two curvatures in 2D and 3D in a single-segment TDCR. Finally, we demonstrate the addressable actuation of two MLMs to further increase the number of achievable curvatures in the single TDCR segment.

This paper is organized as follows. In section II the working principle and the design of the MLM are discussed. The robot prototype design and demonstration is detailed in section III. Section IV presents the experimental evaluation of the MLM and robot prototype. Section V provides a discussion of the experimental results and section VI concludes the paper with proposed future work.

II. Design of the Magnetic Locking Mechanism

In this section, the design and working principle of the MLM are presented. Then, the integration of the MLM with a TDCR segment is discussed.

A. Working Principle of the MLM

The locking mechanism has two main components: the stationary component referred to as the locking mechanism disk, and the moving component referred to as the MLM. The MLM has an on-board magnet, allowing it to be rotated about its central axis through the application of an external magnetic field. This external actuation allows the device to be switched between its locked and unlocked states wirelessly. To actuate the MLM, magnetic torques are employed as these are typically much stronger than magnetic forces. A magnetic torque is produced when the magnetization direction (a.k.a. magnetic dipole moment) of the actuated magnet and the externally applied magnetic field are misaligned. The magnet on the MLM is diametrically magnetized (along a direction perpendicular to its axis of symmetry), thus when an external magnetic field is applied, the MLM rotates about its central axis to align itself with the applied magnetic field. The magnetic torque acting on the MLM is

$$\boldsymbol{\tau} = \boldsymbol{m} \times \boldsymbol{B}, \tag{1}$$

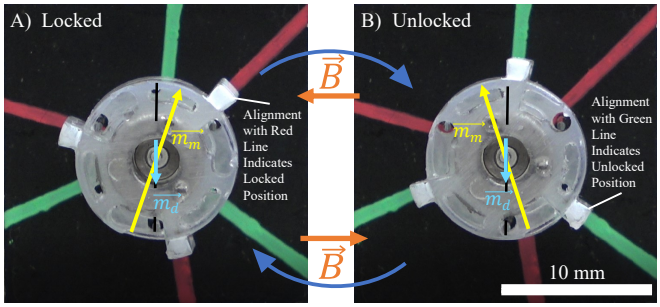

Fig. 2: Locked and unlocked positions of the magnetic spring. $\overrightarrow{m_m}$ is the magnetic dipole moment of the MLM's magnet. $\overrightarrow{m_d}$ is the magnetic dipole moment of the locking mechanism disk's magnet. When the clamping arms (painted white) are in line with the red lines in the background, the MLM is in the locked position. When the clamping arms are in line with the green lines in the background, the MLM is in the unlocked position. A) Magnetic spring in the locked position. B) Magnetic spring in the unlocked position.

where $\boldsymbol{\tau}$ represents the magnetic torque acting on the MLM, $\boldsymbol{m}$ is the magnetic dipole moment of the magnet, and $\boldsymbol{B}$ is the external magnetic field.

To produce pseudo-stable locked and unlocked positions, a magnetic spring is embedded into the MLM. The locking mechanism disk has its own diametrically magnetized ring magnet which fits inside and produces its own torque on the MLM's ring magnet. The MLM rotates to try and align its magnetization direction with that of the inner magnet, creating a spring behaviour between the magnets. When the magnetization direction of the outer magnet is in the opposite direction as that of the inner magnet, the assembly reaches an unstable equilibrium point. Thus, if the MLM is pushed past the unstable equilibrium point in either the clockwise or counter-clockwise direction, it will continue to rotate in that direction to try to align itself with the inner magnet. However, in the MLM, mechanical stops are introduced into slots in the device, to prevent it from fully aligning itself with the inner magnet. It will rather stop rotating once the mechanical stops have reached either end of the slots, which correspond to the mechanism's locked and unlocked positions (Fig. 2). This magnetic spring is included in the MLM design to provide a torque to the MLM which helps it remain in either the locked or unlocked position. As a consequence, once the MLM has been actuated past the unstable equilibrium point, the external magnetic field can be removed as the magnetic spring will push the MLM towards its intended position.

B. MLM Integration on a TDCR

The MLM described in the previous section can be used to produce two curvatures in a single-segment TDCR (Fig. 3). Supporting components in the form of notched secondary backbones are added to a typical TDCR segment such that the MLM can prevent their relative motion. While they have been used to actuate a continuum robot in [19], they play a passive role in this work with the tendons actuating the system. The notched secondary backbones provide a structure onto which the moving portion of the MLM latches.

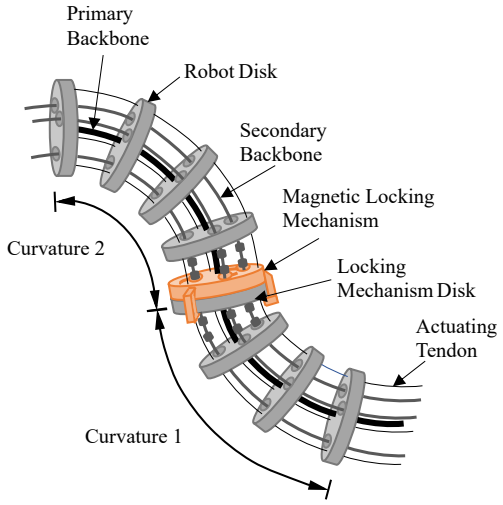

Fig. 3: Graphical depiction of the integration of the MLM on a TDCR segment. The MLM enables two curvatures in a single TDCR segment.

The notches are produced by increasing and decreasing the diameter of the secondary backbones at their center. Three secondary backbones are used in the TDCR segment and the MLM is placed at the middle of the robot segment (Fig. 4). The MLM has six slots, of which three are arc-shaped slots to allow the actuating tendons to pass through the MLM and three are slots which allow the secondary backbones to pass through the MLM (Fig. 4 - Locking Mechanism inset). One side of the secondary backbone slots has a larger opening which allows the secondary backbones to pass through the MLM when the robot is in the unlocked state. To lock the robot, the moving component of the MLM is rotated using an externally applied magnetic field. This causes the narrower side of the slots to slide into the notches, preventing the translation of the secondary backbones.

To enable two curvatures in the robot, it is first bent by manually pulling on the actuating tendons which terminate at the tip of the robot. The MLM is rotated by an external magnetic field, engaging it with the secondary backbones. Since the secondary backbones are fixed at the base of the robot, engaging the MLM causes the proximal half to become locked with its current curvature. The tendons are then actuated to create a second curvature in the distal half of the robot. This principle is validated experimentally on the manually actuated prototype presented in Fig. 1. An S-shaped profile is created in the single-segment continuum robot, which typically requires two robot segments.

III. Enabling Two Curvatures in a TDCR Segment with the MLM

In this section, the MLM is placed on a single-segment TDCR prototype. First, the design of the robot prototype is discussed, followed by a demonstration of the MLM's ability to produce two curvatures in the single-segment TDCR in 2D and 3D space.

TABLE I: Dimensions of the Realized Prototype

Robot Dimensions		MLM Dimensions	
Part	Dimensions	Part	Dimensions
Number of disks	16	Diameter of MLM	10.25 mm
Robot length	240 mm	Diameter of MLM (including clamping arms)	12.75 mm
Disk diameter	10.5 mm	Diameter of locking mechanism disk	10 mm
Disk thickness	2.7 mm	MLM magnet (diametrically magnetized N42 NdFeB ring), outer diameter	1/4"
Primary backbone diameter	0.635 mm	MLM magnet inner diameter	1/8"
Secondary backbone diameter	0.508 mm	MLM magnet height	1/4"
Young's Modulus of the nitinol backbones	50 GPa		

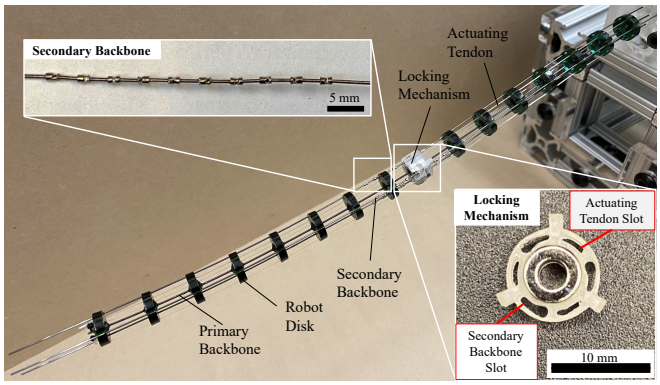

Fig. 4: Magnetic locking mechanism on board the single-segment continuum robot with insets of the top view of the locking mechanism and a secondary backbone.

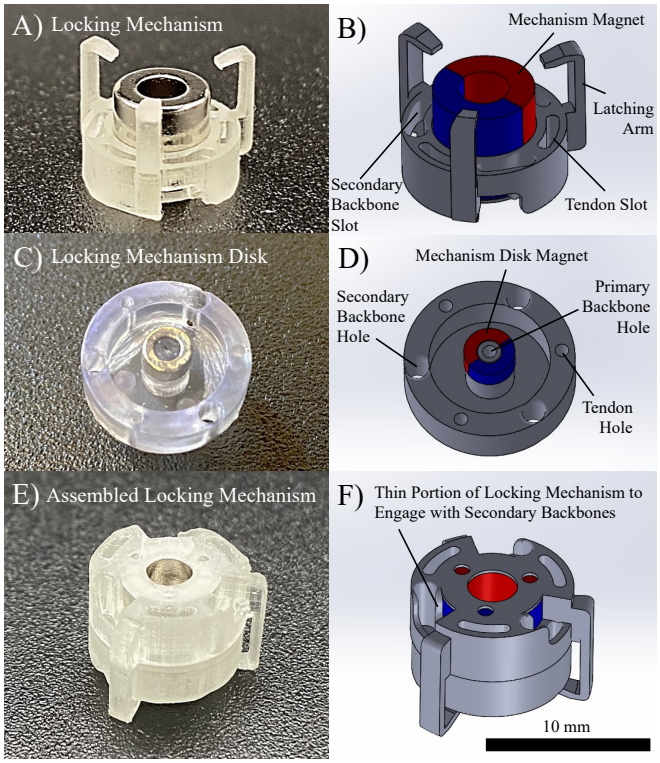

Fig. 5: Magnetic locking mechanism components. A) Magnetic locking mechanism. B) CAD model of the magnetic locking mechanism. C) Locking mechanism disk with which the locking mechanism is paired. D) CAD model of the locking mechanism disk. E) Magnetic locking mechanism assembled with its corresponding disk. F) CAD model of the magnetic locking mechanism assembled with its corresponding disk.

A. Robot Prototype

To demonstrate the MLM's ability to produce two curvatures in a single-segment TDCR, a novel prototype was built. The robot prototype is composed of a primary backbone, three actuating tendons, a MLM, and three secondary backbones (Fig. 4). Its dimensions, which were experimentally chosen based on a trade-off between the robot's stiffness and its maximum bending angle, are tabulated in Table I. The MLM's components are shown in Fig. 5. The MLM pivots about the robot's primary backbone when it is actuated by a magnetic field. There are three clamping arms protruding off the side of the MLM. These arms are used to mechanically constrain the MLM to a robot disk so it does not slide along the robot's backbone and is not repelled by the inner magnet of the magnetic spring. The six slots in the MLM are 4.25 mm from the primary backbone, are placed 60° apart, and each spans 35° of the MLM. The narrower portion of the secondary backbone slots is made thinner to improve its ability to engage with the secondary backbones. The MLM and the locking mechanism disk are 3D printed. The robot disk has larger holes to allow the passage of the secondary backbones, and smaller holes for the actuating tendons. The other robot disks are laser cut from a 2.7 mm thick acrylic sheet using the Epilog Mini 40 Watt laser cutter.

The robot's primary and secondary backbones are made from nitinol wire. At the center of the secondary backbone wire, stainless steel rings are crimped 2.5 mm apart. This creates the notches in the secondary backbones into which the MLM is engaged. Crimping is used as joining methods such as gluing, soldering and welding do not provide sufficiently strong bonds. The robot's actuating tendons are made from fishing line (Orvis SuperStrong Plus, 25lb). To actuate these tendons, a 3D printed manual actuation unit is developed. The robot is mounted into the front of the manual actuation unit, and the actuating tendons are routed over pulleys to reduce the experienced friction. The tendons are manually pulled or released to actuate the robot.

To actuate the MLM, a magnetic field is applied perpendicularly to the magnetization direction of the MLM's magnet and in the magnet plane to rotate the MLM. The magnetic field is produced by an eight-coil electromagnetic actuation system capable of producing maximum fields of 38 mT in all directions. The magnitude and orientation of the magnetic field at the center of the workspace is controlled using the strategy presented in [20]. A linear relationship between the coil currents and the generated magnetic field

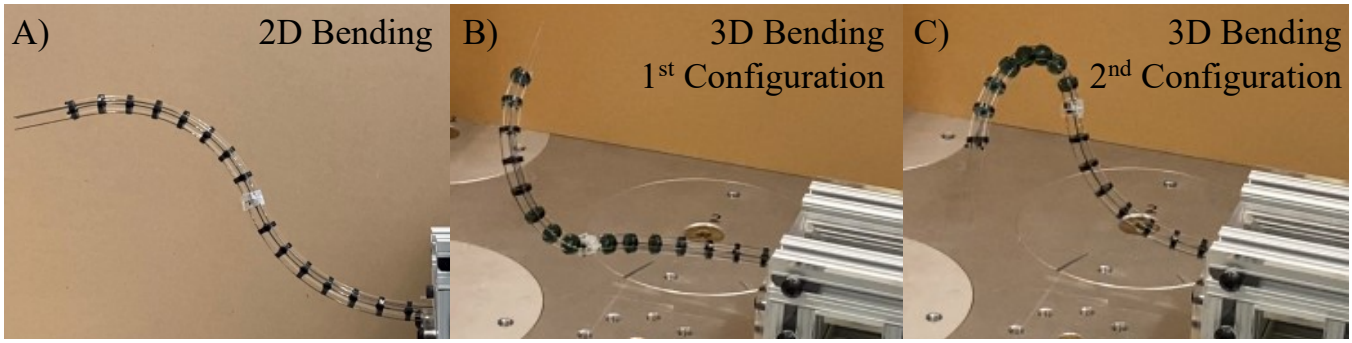

Fig. 6: A) Enabling two curvatures in a single robot segment in two-dimensional space. B) Enabling two curvatures in a single robot segment in three-dimensional space - 1^{st} Configuration. C) Enabling two curvatures in a single robot segment in three-dimensional space - 2^{nd} Configuration.

and its gradients is established and calibrated from field measurements. This relation is then inverted to obtain desired currents, that are met using low level PID control for each coil. At the center of the actuation system's workspace, the error between the specified and produced field is less than 10%.

B. Demonstration of Working Principle

The MLM's ability to produce two curvatures in the robot segment in 2D and 3D space is demonstrated on the robot prototype. The process for achieving two curvatures described in section II-B is used in these demonstrations. The robot is initially bent by manually pulling on the tendons, and a magnetic field is applied perpendicularly to the magnetization direction of the MLM's magnet and in the magnet plane to rotate the MLM and engage it with the secondary backbones. The orientation of the applied field can be specified, which is achieved using the magnetic field control described in section III-A. With the proximal half of the robot locked, the magnetic field is removed, and the distal half is actuated to assume a second curvature. To return the robot to its starting configuration, the tension in the tendons is released and the initial set of tendons are pulled to return the robot to its initial curvature. A field is then applied in the opposite direction of the initially applied field to unlock the MLM. Finally, the robot is returned to its starting position by releasing the tension in the tendons. The robot's ability to achieve two curvatures in 2D and 3D is shown in Fig. 6. For the 3D bending case, the robot assumes two consecutive two-curvature configurations, demonstrating the robot's potential to execute more complex position sequences. The 2D and 3D bending demonstrations are presented in the supplementary video.

IV. Experimental Evaluation

The performance of the MLM and robot prototype is experimentally evaluated. We characterize the locking mechanism in terms of actuation field and holding capacity during tendon actuation. The potential for achieving a greater number of curvatures in a single robot segment by addressably actuating two MLMs is also explored.

A. Field Required for Locking and Unlocking

The goal of this experiment is to ensure that the MLM can be actuated using an external magnetic field when placed onboard the robot prototype. The force acting on the MLM changes when the robot varies its bending angle due to changing tendon tension. Thus, the relationship between the robot bending angle and the magnetic field required to actuate the MLM for the different bending angles is studied.

1) Experimental Set Up: The robot prototype is placed in the workspace of the eight-coil electromagnetic actuation system. While the field produced by the magnetic actuation unit is non-uniform, at the center of its workspace, the effect of the magnetic gradients on the MLM is negligible. To ensure that the MLM is at the center of the workspace, the robot's actuation unit's position is adjusted manually. The locking and unlocking fields are measured for robot bending angles of 0°, 15°, 30°, 45°, 60°, 75°, 90°, 105°, 120°, and 135°. The robot bending angle is defined by the angle between the tangent at the base of the robot's primary backbone and the line passing through the primary backbone base and the robot tip. It is measured using a large laser-cut protractor placed behind the robot (Fig. 7(a)). To reach the desired bending angles, calibrated weights are fixed to the robot's top-most tendon.

Once the desired bending angle is obtained, the secondary backbones are repositioned to ensure that their notches are aligned with the MLM so that it can be engaged. This ensures that only the robot bending angle's effect on the actuating field is considered in this experiment. A magnetic field is then applied along the MLM to engage it with the secondary backbones. The field strength is increased in increments of 0.5 mT until the MLM locks and the field causing locking is recorded. The same process is repeated to unlock the MLM, but with the field applied in the opposite direction. Ten measurements are taken for both the locking and unlocking fields for all robot bending angles considered. The average field strength required for locking and unlocking is finally computed.

2) Results: The average magnetic field required to actuate the MLM for all robot bending angles considered is plotted in Fig. 7(b)). The magnetic field required to actuate the MLM

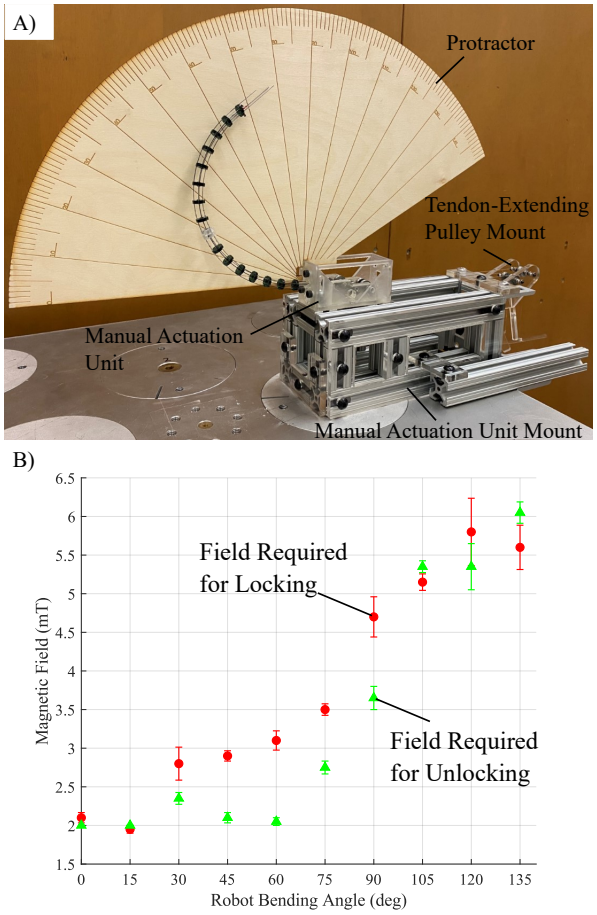

Fig. 7: A) Experimental set up used to measure the magnetic field required to lock and unlock the locking mechanism. B) Average magnetic field required to lock and unlock the locking mechanism for different robot bending angles. The error bars represent the standard error of the measurements.

increases as the robot bending angle increases. The field required to actuate the magnetic locking mechanism for all robot bending angles was relatively weak as it did not surpass 7 mT.

B. Field Required to Unlock a Locked MLM

In this experiment, the field required to unlock the MLM when it is in its loaded state is measured. When the MLM is locked and the distal half of the robot is being actuated, the MLM becomes loaded as the tension applied to the tendons is transmitted to the MLM and the proximal half of the robot. The goal of this experiment is to ensure that the MLM will not become unlocked in its loaded state.

1) Experimental Set Up: When the locking mechanism is loaded, the friction in the MLM increases making it impossible to unlock when the distal half of the robot is being actuated. The MLM is in its least loaded state when the proximal half of the robot is locked and the distal half is straight, i.e. there is no tension in the tendons. Thus, this experiment considers this minimal loading case. The experimental set up is the same as in section IV-A, but with the proximal half of the robot locked and the distal half straight such that there is no tension in the tendons. The robot is initially bent to the desired angle by hanging calibrated weights from the tendons. The secondary backbones are then repositioned to align their notches with the MLM. The MLM is then manually engaged to lock the proximal half of the robot and all tension is released from the tendons. A magnetic field is applied perpendicularly to the MLM's magnetization direction in increments of 0.5 mT until the MLM unlocks or until the field reaches 20 mT. The maximum field of 20 mT is considered sufficiently high as this is more than three times greater than the field required to unlock the MLM measured in section IV-A. This process is repeated five times for each robot bending angle. The bending angles considered for this experiment are from 0° to 105° in intervals of 15°. Higher angles are not explored as it is assumed that the friction in the MLM would be greater, making it more difficult to unlock the mechanism.

2) Results: For bending angles greater than 0°, the loaded MLM stayed locked for actuating fields of up to 20 mT. For the 0° bending case, the MLM unlocked for an average field strength of 18.1 mT. This field is 2.99 times and 3.23 times greater than the maximum unlocking and locking fields presented in section IV-A respectively. Thus, the MLM is unlikely to unlock when in the loaded state, even if a magnetic field were applied. Furthermore, since the magnetic field used to lock and unlock the MLM in section IV-A never exceeded 7 mT, fields of 18.1 mT would not be applied to the system. Thus, even for the 0° bending case, it is not likely that the MLM unlocks.

C. Addressable Actuation of Two MLMs

The TDCR's motion capabilities could be further improved by adding multiple MLMs on board the robot. For example, two MLMs could be used to enable three curvatures in the segment. Since the magnetic field applied to lock and unlock the MLM acts over the robot's entire workspace, the MLMs' magnetic components must be oriented in a way which allows for addressable actuation of multiple MLMs. In this experiment, we investigate the addressable actuation of two MLMs using a global magnetic field.

1) Experimental Set Up: Two MLMs are placed 40 mm apart in the workspace of the electromagnetic actuation system. The magnetization directions of the two MLMs are offset by 90° to allow addressable actuation of both mechanisms. One of the MLMs is placed on a fixed insert which does not move. The second MLM is placed on different inserts with varying inclination angles of 0°, 30°, 60°, and 90°. These inclined inserts are also placed on a rotating disk (Fig. 8). For each inclined insert, the disk is rotated by 0°, 30°, 60°, and 90° relative to the fixed MLM. By placing the second MLM on the inclined and rotatable inserts, the relative orientation between the two MLMs mimicks that of two MLMs placed on a single-segment TDCR. For each inclined insert and rotation angle, a magnetic field is applied to actuate one of the two MLMs. The orientation of the magnetic field is then changed to actuate the other MLM.

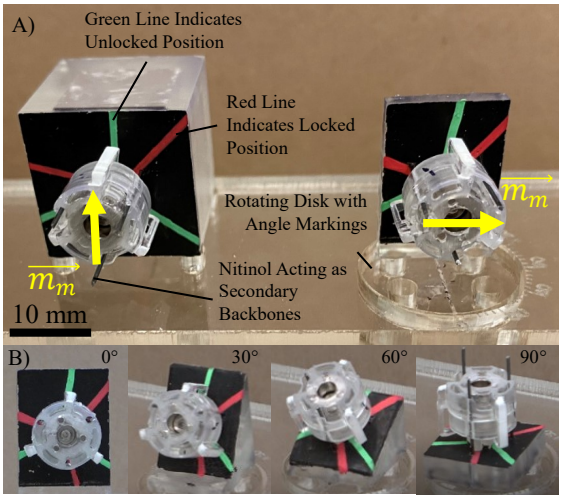

Fig. 8: A) Experimental set up for the addressable actuation of two MLMs. The yellow arrows represent the magnetization directions of the locking mechanisms ($\overrightarrow{m_m}$). When the clamping arms (painted white) are in line with the red lines in the background, the MLM is in the locked position. When the clamping arms are in line with the green lines in the background, the MLM is in the unlocked position. The locking mechanism on the right is placed on an inclined insert which can be rotated relative to the left locking mechanism. B) Inserts on which the right locking mechanism is placed with inclination angles of 0°, 30°, 60°, and 90°.

2) Results: For every inclined insert and rotation angle considered, it was shown that two MLMs could be addressably actuated using a global magnetic field. In some cases, a small movement was observed in the unactuated MLM, however, not enough to trigger the locking mechanism. Choosing an appropriate field orientation to actuate a single MLM is not trivial. This will be discussed in section V. The addressable actuation of two MLMs with a relative inclination and rotation angles of 0° is shown in the supplementary video.

V. Discussion

A. Magnetic Field

It was shown that the MLM is easily actuated with a relatively weak external magnetic field. The magnitude of the field required increases with the robot bending angle, likely caused by a greater portion of the secondary backbones and actuating tendons being in contact with the MLM for larger bending angles resulting in increased friction. The slight deviations from the trend could be caused by misalignment between the secondary backbone notches and the MLM. The friction between the MLM and the locking mechanism disk may have also changed between measurements due to wear or relative motion. In addition, the field required to unlock the MLM is smaller than the field required for locking. This may be caused by the size differences at either end of the secondary backbone slots which result in different magnitudes of experienced frictional forces.

Additionally, the MLM's use is not limited to the specialized magnetic actuation system used in this work. The field required to actuate the MLM was below 7 mT for all robot bending angles, allowing most magnetic actuation units in literature to be used instead. For example, the Octomag [20] can produce fields above 20 mT while the Stereotaxis Niobe and Aeon Phocus [21], [22] can produce fields up to 80 mT.

B. Locking Mechanism

The experiments also showed that the MLM did not undesirably unlock even when large magnetic fields were applied. Since the friction in the MLM is high when in its loaded state, it is unlikely that the MLM becomes unlocked when the distal half of the robot is actuated. However, it may be possible that the MLM unlocks in the presence of significant torsion. If the robot experiences external loading or if a specific combination of tendons are actuated, the resulting torsion could unlock the MLM. In future work, experimental validation must be performed to ensure that the MLM stays locked under different loading conditions. In the experiments, the locked MLM did not unlock for fields of up to 20 mT (18.1 mT for the 0° bending case). Therefore, fields with these magnitudes could be used to freely actuate a second MLM on the robot, where the friction in the first loaded MLM would prevent it from unlocking.

C. Addressable Actuation

Next, it was shown that two MLMs could be addressably actuated, thus demonstrating the potential for multiple locking mechanisms on a single robot. Two locking mechanisms could be used to produce three curvatures in a single segment, or four on a two-segment robot. In some of the considered cases, a small movement was observed in the unactuated MLM, however, not enough to trigger the locking mechanism. This could be caused by misalignment of the magnetization direction of the MLMs or by the application of out of plane torques (i.e. not about the axis of rotation) which would not cause the MLMs to lock or unlock. Furthermore, placing the MLMs 40 mm apart verifies that magnetic interaction between MLMs does not prevent their independent actuation.

Choosing the field orientation to actuate multiple MLMs is not trivial as its easier for certain relative MLM orientations. For example, when the relative inclination and rotation angles between the MLMs are both 0°, one MLM can be actuated by simply applying a field along the other MLM's magnetization direction. However, this can be challenging when, for example, the relative inclination and rotation angles between the two MLMs are both 90°. Applying a field along the unactuated MLM's magnetization direction will not cause the desired MLM to be actuated as the field would be along its rotation axis. In such cases, the friction in the mechanism can be leveraged. The field can be oriented to produce a larger torque on the actuated MLM and a smaller one on the other MLM such that it is not sufficient to overcome the friction in the latter device, thereby preventing it from being actuated. In practice, the above would require tracking of the MLM orientations and positions such that the magnetic field can be oriented in a way which actuates a single MLM at a time. In future work, magnetic sensors could be embedded in the robot to obtain their pose [23]. A model could be

derived to determine the field orientation which produces a larger torque acting on the actuated MLM based on the information obtained from the magnetic sensing.

D. Limitations

Our experiments revealed some limitations of the proposed design, mainly due to manual manufacturing and prototyping. First, the robot can only be locked in specific configurations due to the discrete placement of the rings on the secondary backbones. Its performance could be improved if the distance between notches was reduced. The spacing of the rings on the secondary backbones also creates some slack in the robot since the locking mechanism is slightly thinner than the ring spacing. Some shifting was also observed in the robot when the MLM was actuated. This could be easily eliminated by using smaller actuating fields or a smaller magnet on the MLM. While the magnetic field had a small influence on the robot's shape, future work will focus on developing a model to study the effects of the applied magnetic field on robot deformation.

VI. Conclusion

In this work, two curvatures were enabled in a single-segment TDCR through the use of a novel MLM. To extend the benefits of the MLM, it was shown that two of the developed MLMs could be addressably actuated, demonstrating the potential of achieving a greater number of curvatures in a single TDCR segment. In future work, a kinematic model of the robot will be developed to further study and analyze the proposed design. A model could be used to determine the required tendon input forces needed to generate desired robot shapes and to investigate the workspace of the novel continuum robot. Automating the actuation will eliminate the vibrations observed due to manual actuation, and enable linear advancement and retraction of the robot. Using the MLM to achieve follow-the-leader motion will also be investigated. Future work will focus on device miniaturization by using custom magnets in the MLM. Finally, the stiffness increase observed in the locked portion of the robot will be experimentally characterized.

VII. Acknowledgement

The authors would like to thank Adam Schonewille for the design and development of the magnetic actuation system used in this work.

References

[1] J. Burgner-Kahrs, D. C. Rucker, and H. Choset, "Continuum robots for medical applications: A survey," *IEEE Transactions on Robotics*, vol. 31, no. 6, pp. 1261–1280, 2015.

[2] P. Rao, Q. Peyron, S. Lilge, and J. Burgner-Kahrs, "How to Model Tendon-Driven Continuum Robots and Benchmark Modelling Performance," *Frontiers in Robotics and AI*, vol. 7, 2021.

[3] J. Starke, E. Amanov, M. T. Chikhaoui, and J. Burgner-Kahrs, "On the merits of helical tendon routing in continuum robots," in *IEEE International Conference on Intelligent Robots and Systems*, 2017, pp. 6470–6476.

[4] L. T. Gan, L. H. Blumenschein, Z. Huang, A. M. Okamura, E. W. Hawkes, and J. A. Fan, "3D electromagnetic reconfiguration enabled by soft continuum robots," *IEEE Robotics and Automation Letters*, vol. 5, no. 2, pp. 1704–1711, 2020.

[5] A. Gao, H. Liu, Y. Zhou, Z. Yang, Z. Wang, and H. Li, "A cross-helical tendons actuated dexterous continuum manipulator," in *IEEE International Conference on Intelligent Robots and Systems*, 2015, pp. 2012–2017.

[6] K. Oliver-Butler, J. Till, and C. Rucker, "Continuum Robot Stiffness under External Loads and Prescribed Tendon Displacements," *IEEE Transactions on Robotics*, vol. 35, no. 2, pp. 403–419, 2019.

[7] M. Giorelli, F. Renda, M. Calisti, A. Arienti, G. Ferri, and C. Laschi, "A two dimensional inverse kinetics model of a cable driven manipulator inspired by the octopus arm," in *Proceedings - IEEE International Conference on Robotics and Automation*, 2012, pp. 3819–3824.

[8] H. Liu, Z. Ji, J. Li, Y. Zhou, C. Wang, and P. Ba, "A S shape continuum robot with a single actuation structured by NiTi slices," *IEEE International Conference on Robotics and Biomimetics, ROBIO*, pp. 401–405, 2017.

[9] M. Plooij, G. Mathijssen, P. Cherelle, D. Lefeber, and B. Vanderborght, "Lock your robot: A review of locking devices in robotics," *IEEE Robotics and Automation Magazine*, vol. 22, no. 1, pp. 106–117, 2015.

[10] C. Yang, S. Geng, I. Walker, D. T. Branson, J. Liu, J. S. Dai, and R. Kang, "Geometric constraint-based modeling and analysis of a novel continuum robot with Shape Memory Alloy initiated variable stiffness," *The International Journal of Robotics Research*, vol. 39, no. 14, pp. 1620–1634, 2020.

[11] S. Wang, R. Zhang, D. A. Haggerty, N. D. Naclerio, and E. W. Hawkes, "A Dexterous Tip-extending Robot with Variable-length Shape-locking," *IEEE International Conference on Robotics and Automation*, pp. 9035–9041, 2020.

[12] C. Bishop, M. Russo, X. Dong, and D. Axinte, "A Novel Under-actuated Continuum Robot With Shape Memory Alloy Clutches," *IEEE/ASME Transactions on Mechatronics*, pp. 1–12, 2022.

[13] B. Kang, R. Kojcev, and E. Sinibaldi, "The First Interlaced Continuum Robot, Devised to Intrinsically Follow the Leader," *PLOS ONE*, vol. 11, 2016.

[14] C. Sun, L. Chen, J. Liu, J. S. Dai, and R. Kang, "A hybrid continuum robot based on pneumatic muscles with embedded elastic rods," *Proceedings of the Institution of Mechanical Engineers, Part C: Journal of Mechanical Engineering Science*, vol. 234, no. 1, pp. 318–328, 2020.

[15] P. Wang, S. Guo, F. Zhao, X. Wang, and M. Song, "Follow-the-leader deployment of the interlaced continuum robot based on the unpowered lock mechanism," in *Intelligent Robotics and Applications. Lecture Notes in Computer Science*, vol. 13015, 2021, pp. 448–459.

[16] S. Zuo, N. Ymanaka, K. Masamune, H. Liao, K. Matsumiya, and T. Dohi, "MRI compatible rigid-flexible outer sheath device using pneumatic locking mechanism for endoscopic treatment," in *Proc. 7th Asian-Pacific Conf. on Medical and Biological Engineering*, 2008, pp. 210–219.

[17] B. J. Nelson, S. Gervasoni, P. W. Chiu, L. Zhang, and A. Zemmar, "Magnetically Actuated Medical Robots: An in vivo Perspective," *Proceedings of the IEEE*, vol. 110, no. 7, 2022.

[18] C. Forbrigger, A. Schonewille, and E. Diller, "Tailored magnetic torsion springs for miniature magnetic robots," in *IEEE International Conference on Robotics and Automation*, 2021, pp. 7182–7188.

[19] L. Wang, G. Del Giudice, and N. Simaan, "Simplified kinematics of continuum robot equilibrium modulation via moment coupling effects and model calibration," *Journal of Mechanisms and Robotics*, vol. 11, no. 5, 2019.

[20] M. P. Kummer, J. J. Abbott, B. E. Kratochvil, R. Borer, A. Sengul, and B. J. Nelson, "Octomag: An electromagnetic system for 5-DOF wireless micromanipulation," *IEEE Transactions on Robotics*, vol. 26, no. 6, pp. 1006–1017, 2010.

[21] F. Carpi and C. Pappone, "Stereotaxis Niobe® magnetic navigation system for endocardial catheter ablation and gastrointestinal capsule endoscopy," *Expert Review of Medical Devices*, vol. 6, no. 5, pp. 487–498, 2009.

[22] C. Chautems, A. Tonazzini, Q. Boehler, S. H. Jeong, D. Floreano, and B. J. Nelson, "Magnetic continuum device with variable stiffness for minimally invasive surgery," *Advanced Intelligent Systems*, vol. 2, no. 6, p. 1900086, 2020.

[23] H. Guo, F. Ju, Y. Cao, F. Qi, D. Bai, Y. Wang, and B. Chen, "Continuum robot shape estimation using permanent magnets and magnetic sensors," *Sensors and Actuators, A: Physical*, vol. 285, pp. 519–530, 2019.